A Grid Lifetime Model for a 3-Grid Ion Engine*†

Masakatsu Nakano
Japan Science and Technology Corporation
Kakuda Space Propulsion Laboratory
National Aerospace Laboratory
1 Koganesawa, Kimigaya, Kakuda-shi, Miyagi
981-1525 Japan
+81-224-68-3926
nakano@kakuda-splab.go.jp

IEPC-01-84

A grid lifetime model is presented for the lifetime estimation of a 3-grid ion engine system. The failure mechanism considered in the model is electron backstreaming due to charge exchange ion erosion, which is fatal to the operation of the ion engine. The process which will be ended with electron backstreaming is described as follows: 1) charge exchange ion erosion enlarges accel grid hole diameter, 2) the enlarged accel grid hole diameter decreases the negative potential between the screen and accel grids, and 3) the negative potential becomes too small to expel the neutralizing electrons away from the discharge chamber. The above process is modeled with the space-charge-limited current density law and a newly introduced parameter called extended effective acceleration length. The characteristic of the model is that lifetime strongly depends on beam current and accel grid voltage. An evaluation was made to validate the model using a computer program and showed that the model agreed quite well with simulations and gave good scaling for grid lifetime.

Introduction

Since ion engines provide high specific impulse and high thrust efficiency, and the scaling laws have been well established, the ion engine is being put to practical use in Japan, the U.S. and Europe.[1-3] To compensate for low thrust acceleration and meet a variety of requirements for future space missions, the required lifetime of ion engine system is quite long, which ranges from several months to over several years. Therefore, the assessment and establishment of such long periods of operation of ion engine system is immediate problems to be worked on.

The ion engine system consists of many components with limited lifetime due to their inherent failure modes.[4,5] One of the failure modes is known as a grid erosion caused by charge exchange ions. Unfortunately grid erosion cannot be stopped since the production of charge exchange ions constantly occurs during the operation of the ion engine. Thus, accurate evaluations of grid erosion are critical to the successful assessments of the lifetime of ion engine.

Since performing actual life-tests requires devastating time, numerical simulation is preferred in most of the parametric studies. Numerical simulation is a helpful and powerful tool, however it does not provide a clear image of lifetime scaling compared with that of analytical models.

In this paper, a grid lifetime model is presented for the lifetime estimation of a 3-grid ion engine system. Since most of the lifetime simulations so far ended up with electron backstreaming, which is fatal to ion beam acceleration,[6-8] the model is constructed to provide a lifetime scaling of the ion engine, which was resulted from such electron backstreaming phenomena. The life-limiting process, which would be ended with electron backstreaming was modeled using the space-charge-limited current density law and a newly introduced parameter called extended effective acceleration length.

* Presented as Paper IEPC-01-84 at the 27th International Electric Propulsion Conference, Pasadena, CA, 15-19 October, 2001.

Modeling

Life-limiting Process

The life-limiting process is described as follows: 1) charge exchange ion erosion enlarges accel grid hole diameter, 2) the enlarged accel grid hole diameter decreases the negative potential between the screen and accel grids, and 3) the negative potential becomes too small to keep neutralizing electrons away from the discharge chamber. The beginning of life (BOL) and end of life (EOL) of the process are shown in Figs.1 (a) and (b), respectively. The saddle point voltage at BOL is negatively high enough to expel neutralizing electrons however it cannot expel the electrons at EOL.

Assumption

The basic idea of the model is the extension of the effective acceleration length used in the space-charge-limited current density law and the assumptions made below.

- One-dimensional potential distribution towards the axial direction
- Beam current is kept constant during operation
- The screen grid, accel grid and decel grid voltages are constant during operation
- Grid life is reached at the time when the saddle point potential becomes 0 V
- Most of the accel grid erosion is due to energetic charge exchange ions created between the screen and accel grids - Assumption (1)
- Grid mass loss occurs uniformly on the inner surface of the accel grid and develops towards the radial direction - Assumption (2)
- Beam current density is not depending on the enlargement of accel grid hole diameter. - Assumption (3). (This assumption is derived from the fact that the experiments by Aston et al. showed that the variation of accel grid hole diameter had little effect on beam divergence angle.[9] From this it is assumed that ion beam profile and beam cross sectional area do not change during the operation even if the accel grid hole diameter is enlarged by erosion.)

Formulation

It is known that the ion beam flow between the screen and accel grids is well modeled with the space-charge-limited current density law and the effective acceleration length.[9,10] Since most of the ions flow

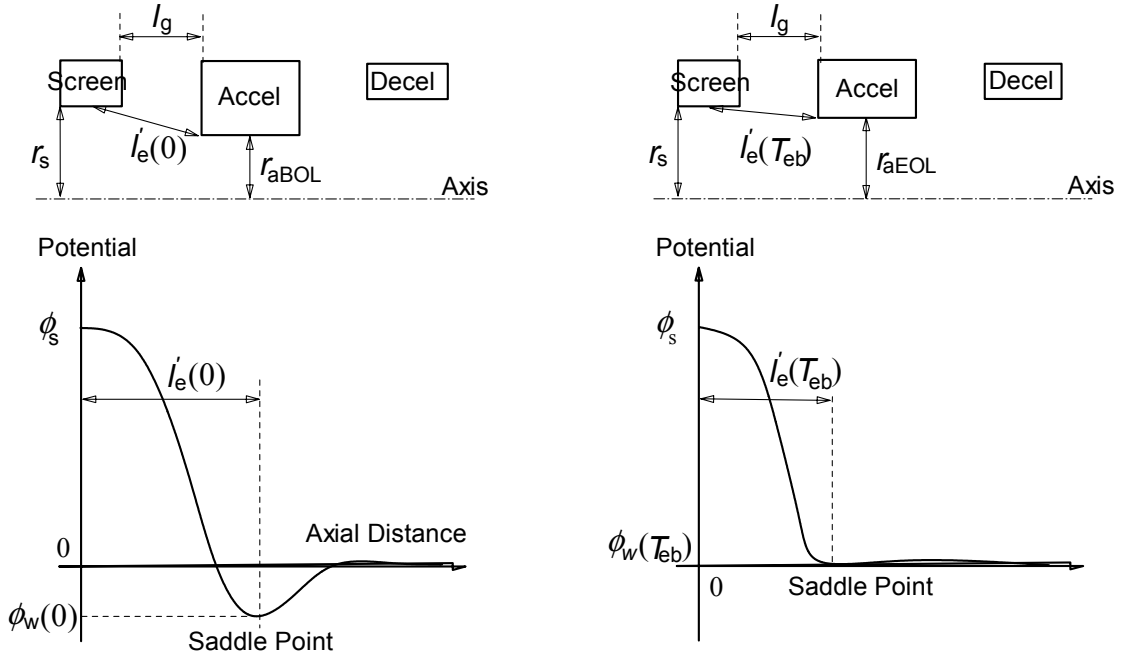

(a) BOL (b) EOL

Figure 1. The grid shapes and potentials on the axis at (a) BOL and (b) EOL

nearby the grid axis due to the focusing of ion beams, it is appropriate to use the saddle point potential $\phi_w(t)$ rather than the accel grid potential ϕ_a for the following equation,

$$J_{sc}=\frac{4}{9}\varepsilon_0\sqrt{\frac{2e}{M}}\frac{(\phi_s-\phi_w(t))^{2/3}}{l_e^2(t)} \quad (1)$$

where J_{sc} is a space-charge-limited current density, ε_0 is the permittivity of free space, e is the electron charge, M is the propellant molecular mass, ϕ_s is the screen grid potential, and $l_e(t)$ is the effective acceleration length. In case that ion beam flow is close to the space-charge-limited, beam current density J_B is well modeled as below using Eq.(1).

$$J_B\approx J_{sc}=\frac{4}{9}\varepsilon_0\sqrt{\frac{2e}{M}}\frac{(\phi_s-\phi_w(t))^{2/3}}{l_e'^2(t)} \quad (2)$$

$$l_e'(t)=\sqrt{(t_s/2+l_g)^2+(r_s-r_a(t))^2} \quad (3)$$

where t_s is a screen grid thickness, l_g is a screen-to-accel grid separation, and r_s and $r_a(t)$ are the screen and the accel grid hole radius respectively. Here a new parameter called extended effective acceleration length l_e' is introduced to consider the effect of the enlargement of the accel grid hole diameter (Fig.1.) From Assumption (3), Eqs.(2) and (3), an equation shall be given,

$$\frac{(\phi_s-\phi_w(t))^{3/2}}{l_e'^2(t)}=\frac{(\phi_s-\phi_w(0))^{3/2}}{l_e'^2(0)} \quad (4)$$

Since the saddle point potential becomes 0 V at EOL, Eq.(4) gives

$$r_{aEOL}=\sqrt{\left(\frac{\phi_s}{\phi_s-\phi_w(0)}\right)^{3/2}\left[(t_s/2+l_g)^2+(r_s-r_{aBOL})^2\right]-(t_s/2+l_g)^2} \quad (5)$$

where r_{aBOL} and r_{aEOL} are the accel grid hole radius at BOL and EOL, respectively. Equation (5) suggests that the accel grid hole radius at EOL can be estimated from the grid geometry and the saddle point potential of a specified acceleration system at BOL.

If the accel grid hole radius can be expressed with a function of operating time t, the electron backstreaming time of a specified acceleration system T_{eb} can be obtained solving $r_a(T_{eb}) = r_{aEOL}$. The explicit expression of $r_a(t)$ is given by considering the variation of accel grid hole radius with time.

Table 1. Simulation parameters. *Beam currents are specified to be the same as that of the Case #3.

Case #	NP/H, A/V$^{1.5}$	ϕ_a, V
1	1.60×10^{-9}	-300
2	1.80×10^{-9}	-300
3	2.00×10^{-9}	-300
4	2.20×10^{-9}	-300
5	2.40×10^{-9}	-300
6	2.18×10^{-9}	-200
7	2.09×10^{-9}	-250
8	1.92×10^{-9}	-350
9	1.84×10^{-9}	-400

Since the grid mass loss rate strongly depends on the accel grid beam current per hole i_a and the sputtering rate of the material, and since the sputtering rate is well modeled to be in proportion to the impact energy of the ion E_{CE},[11] the grid mass loss rate is modeled to be in proportion to i_aE_{CE}. From the analogy of the space-charge-limited current density law, $E_{CE}=e(\phi-\phi_a)\propto J_B^{2/3}\propto i_B^{2/3}$ can be derived, where i_B is a beam current per hole. Thus the grid mass loss rate is given in proportion to $i_a i_B^{2/3}$. (The validity of this can be confirmed by checking linear dependence of Δm_a on $i_a i_B^{2/3} T_{eb}$, which will be examined in the following section.) If the accel grid inner surface is eroded uniformly and the radius is increased, the accel grid hole radius is expressed as,

$$r_a(t)=\sqrt{r_{aBOL}^2+k i_a i_B^{2/3} t} \quad (6)$$

where k is a parameter to consider the grid geometry and physical constants. From Eqs.(5) and (6), the electron backstreaming time is given as follows,

$$T_{eb}=\frac{\left(r_s-\sqrt{\left(\frac{\phi_s}{\phi_s-\phi_w(0)}\right)^{3/2}\left[(t_s/2+l_g)^2+(r_s-r_{aBOL})^2\right]-(t_s/2+l_g)^2}\right)^2-r_{aBOL}^2}{k i_a i_B^{2/3}} \quad (7)$$

Taking a ratio to delete k, the following equation is obtained.

$$\frac{T_{eb}}{T_{eb0}}=\frac{\left(r_s-\sqrt{\left(\frac{\phi_s}{\phi_s-\phi_w(0)}\right)^{3/2}\left[(t_s/2+l_g)^2+(r_s-r_{aBOL})^2\right]-(t_s/2+l_g)^2}\right)^2-r_{aBOL}^2}{\left(r_s-\sqrt{\left(\frac{\phi_{s0}}{\phi_{s0}-\phi_{w0}(0)}\right)^{3/2}\left[(t_s/2+l_g)^2+(r_s-r_{aBOL})^2\right]-(t_s/2+l_g)^2}\right)^2-r_{aBOL}^2}\times\left(\frac{i_{a0}}{i_a}\right)\left(\frac{i_{B0}}{i_B}\right)^{2/3} \quad (8)$$

Table 2. Lifetime parameters at EOL

	Simulation					Model
Case #	T_{eb}, hrs	I_a, μA	Δm_a, mg	$\Delta m_{aSA}/\Delta m_a$	r_{aEOL}/r_{aBOL} Eq.(9)	r_{aEOL}/r_{aBOL} Eq.(5)
1	35750	0.86	3.17	0.85	1.32	1.10
2	28000	0.98	3.04	0.86	1.31	1.09
3	24500	1.12	3.05	0.88	1.31	1.09
4	21000	1.26	2.98	0.84	1.30	1.09
5	19000	1.39	2.98	0.88	1.30	1.09
6	1750	1.45	0.32	0.91	1.04	1.02
7	11250	1.22	1.63	0.90	1.17	1.05
8	42750	1.05	4.61	0.85	1.44	1.14
9	83500	0.98	7.24	0.82	1.64	1.19

Since beam current density actually becomes maximum at the part of the grid center, i_a and i_B should be modified to $I_a/f_a(I_a)$ and $I_B/f_B(I_B)$ to yield maximum beam currents per hole, where I_a is the accel grid current, I_B is the beam current, and f_a and f_B are beam flatness parameters of I_a and I_B, respectively. It should be noted that all parameters in the model are given beforehand or are obtainable either by calculations or measurements.

Sample Calculations

Since the number of lifetime experiments having been conducted so far are too limited to provide us with parametric lifetime data, an evaluation was performed by a numerical code.[8] The code calculates variations of erosion with time by solving electrostatic potentials, tracking ion trajectories, evaluating the amount of grid material removed from the grid surface and determining its shape. The following parameters at EOL were obtained for MUSES-C ion engine system[12]

- Electron backstreaming time - T_{eb}
- Accel grid current averaged by time - I_a
- Accel grid mass loss - Δm_a
- Fraction of accel grid mass loss due to charge exchange ions created over 0 V region upstream of the accel grid - $\Delta m_{aSA}/\Delta m_a$
- The ratio of accel grid radius between EOL and BOL - r_{aEOL}/r_{aBOL}

The grid geometry and operating point data used for calculation are given as follows. The screen, accel and decel grid hole diameters are 3.0 mm, 1.8 mm and 2.6 mm, respectively. The thickness of each grid is 1.0

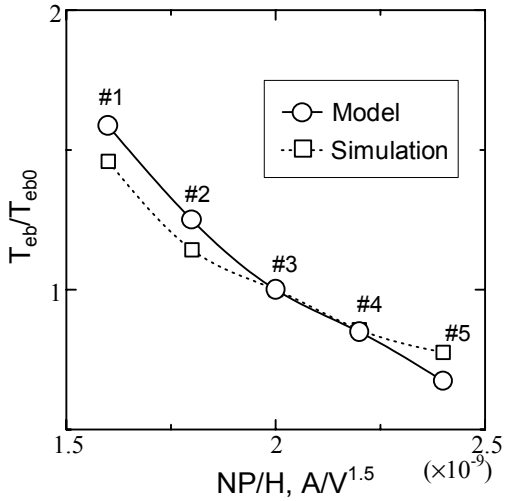

Figure 2. Comparison of lifetimes in different beam currents

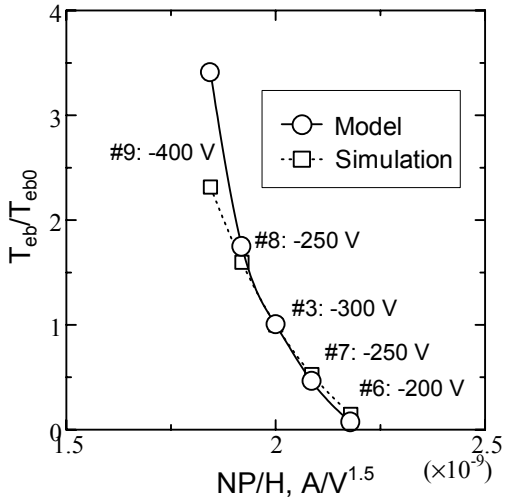

Figure 3. Comparison of lifetimes in different accel grid voltages

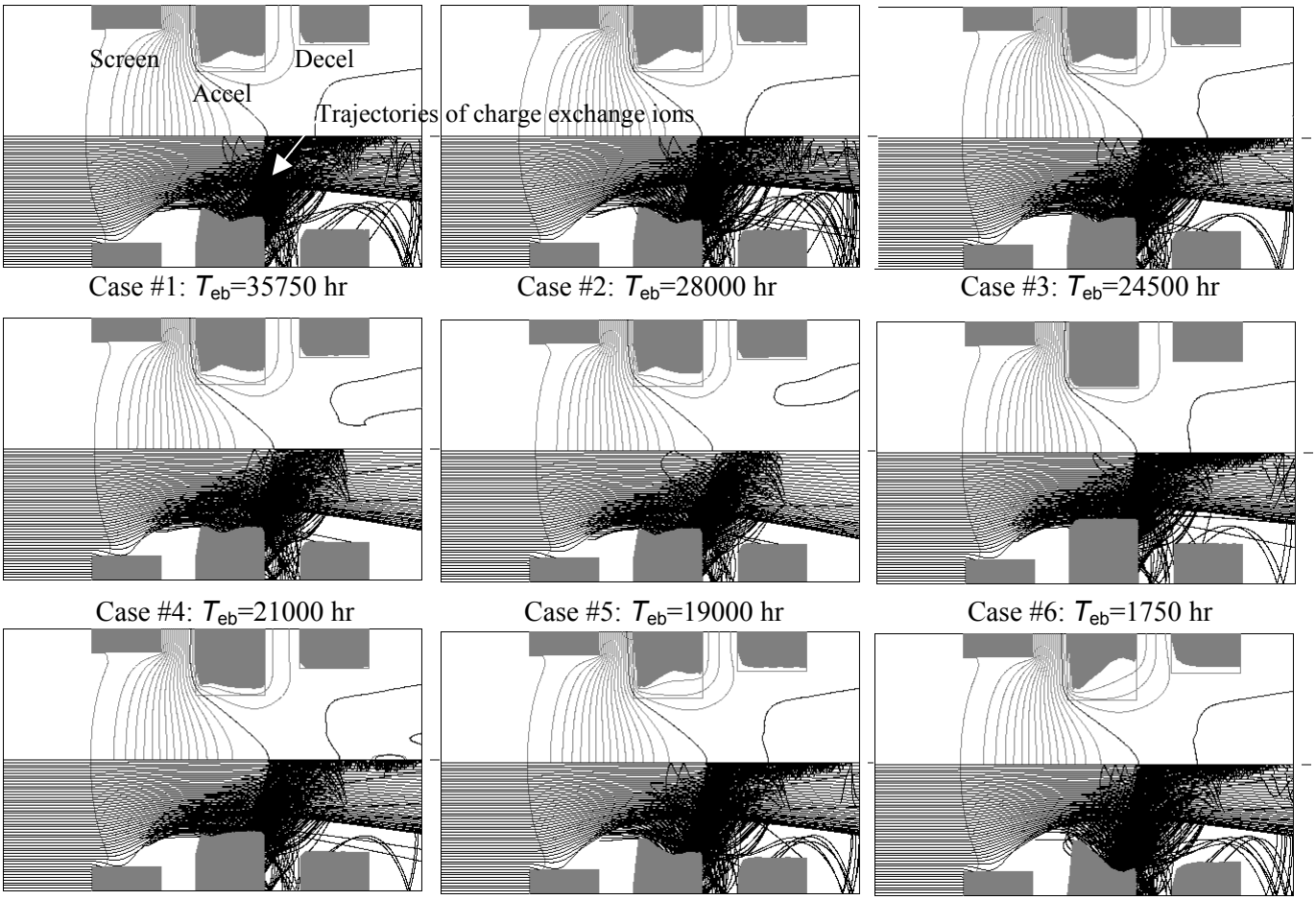

Case #1: T_{eb}=35750 hr Case #2: T_{eb}=28000 hr Case #3: T_{eb}=24500 hr

Case #4: T_{eb}=21000 hr Case #5: T_{eb}=19000 hr Case #6: T_{eb}=1750 hr

Case #7: T_{eb}=11250 hr Case #8: T_{eb}=42750 hr Case #9: T_{eb}=83500 hr

Figure 4. Grid shapes and ion beam trajectories at EOL.

mm. The separation distances of the screen-to-accel and accel-to-decel grids are 0.5 mm, respectively. The screen grid and decel grid potentials are 1500 V and –30 V, respectively. The propellant utilization efficiency η_u is 0.67. The grid material is a C/C composite.

In Table 1, the sets of input parameters for the simulation are tabulated. The lifetime dependence on beam current was examined in the Case #1 to #5 with same accel grid voltage of –300 V, and lifetime dependence on accel grid voltage was examined in the Case #6 to #9 with the same beam current as in the Case #3 (5.5×10^{-4} A.) For the sake of simplicity, one set of grid holes was calculated. The leaking neutral atom density distribution was calculated under the condition of the Case #3 and η_u=0.67. This neutral atom density distribution was used for all other calculations. Boltzmann distribution of electron temperature T_e was selected for electron density distribution. The electron backstreaming time in simulation was defined as the time when the saddle point potential becomes $-kT_e/e$. The electron temperature was assumed to be 5 eV.

In Table 2, all the lifetime parameters at EOL are shown. For comparison, the ratio of accel grid hole radii between EOL and BOL was evaluated using the equation

(9)

where t_a is accel grid thickness and γ is a specific weight of the grid material.

$$r_{aEOL}=\sqrt{r_{aBOL}^2+\frac{\Delta m_a}{\pi t_a \gamma}}$$

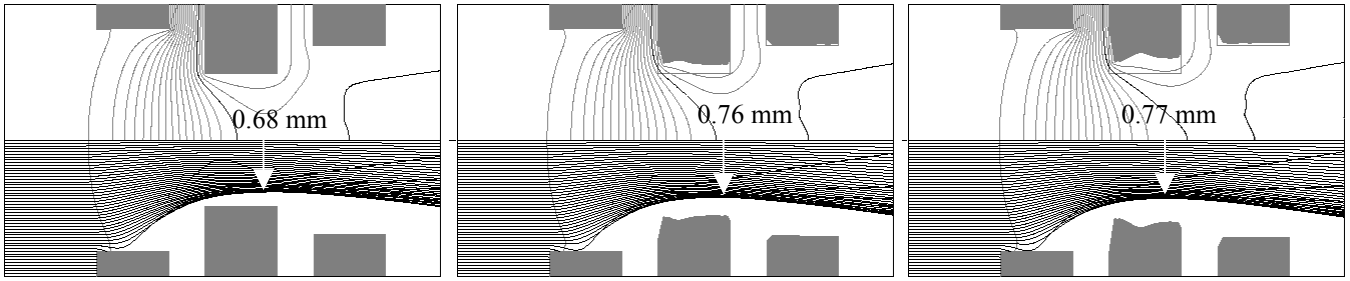

(a) BOL (b) MOL (c) EOL

Figure 5. Variations of ion beam profiles with time in the Case #3.

Beam Current Dependence

Figure 2 shows a comparison of lifetime curves obtained by the simulation and the model. A reference point was provided by the parameters with subscripts of 0 in Eq.(9), which were from the Case #3 , and all data were plotted against normalized perveance per hole. The figure shows that the lifetime curve predicted by the model agrees quite well with the simulation.

As shown in Table 2, the calculated values of r_{aEOL}/r_{aBOL} from Eq.(5) were around 1.1 and agreed qualitatively well with the simulated values, around 1.3. The calculated values of $\Delta m_{aSA}/\Delta m_a$ were around 0.84 to 0.88, which were close to 1. The most of the accel grid erosion causes due to the charge exchange ions created between the screen and accel grids. –This is confirming the Assumption (1).

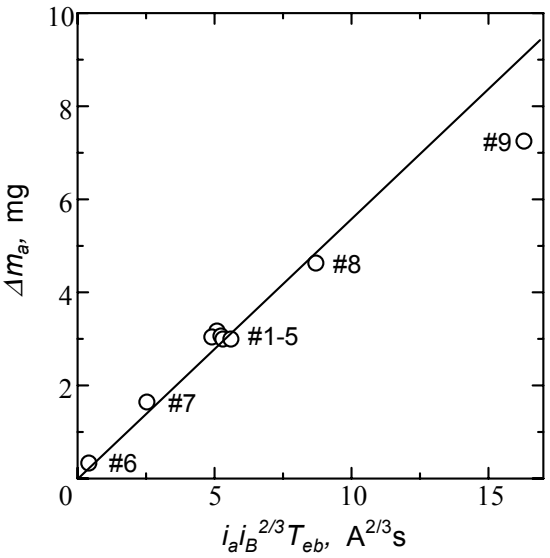

Figure 6. Dependence of grid mass loss on $i_a i_B^{2/3} T_{eb}$

Shown in Figure 4 are the figures of grid shapes, potential distributions and ion beam trajectories at EOL. In the figures, the potentials are shown in the upper and the ion beam trajectories in the lower. The trajectories running downstream from the discharge chamber are the ones of mainstream ions and the trajectories near the accel grids are the ones of charge exchange ions. (Here only trajectories of the ions that impinge on the accel grid were drawn.) From the figures, it is confirmed that most of the erosion occurs on the inner face of the accel grid and develops towards the radial direction by the impingement of charge exchange ions created between the screen and accel grids. These facts prove that Assumptions (1) and (2) are valid.

Shown in Figure 5 are the variations of ion beam profiles with time for the Case #3 conditions. The beam diameters at the most focused positions at BOL, MOL and EOL are 1.36 mm, 1.52 mm and 1.54 mm, respectively. The ratio of beam cross sectional areas between MOL and BOL (in the former half of the operation) is 1.24, and the ratio between EOL and MOL (in the latter half of the operation) is about 1.05. Although Assumption (3) was not exactly supported in the former half of the operation, it was supported in the latter half of the operation with good precision.

Dependence on Accel Grid Potential

The lifetime dependence on accel grid voltage was investigated by changing the accel grid voltage from –200 V to –400 V without changing beam current. The lifetime curves are shown in Figure 3 using parameters of the Case #3 for setting a reference point. The curve for the model shows a very good agreement with that of the simulation. In Table 2, the calculated values of

r_{aEOL}/r_{aBOL} from Eq.(9) were around 1.02 to 1.19 and agreed well with the simulated values in low negative voltage (1.04 and 1.17) however they agreed poorly in high negative voltage (1.44 and 1.64). The calculated values of $\Delta m_{aSA}/\Delta m_a$ were around 0.82 to 0.91, which are close to 1. This is confirming the Assumption (1).

Dependence of Grid Mass Loss on Beam Currents

Shown in Figure 6 are the values of Δm_a for $i_a i_B^{2/3} T_{eb}$, which were obtained by the simulation. The figure shows that they were plotted almost linearly. This indicates that the grid mass loss is well modeled so as to be in proportion to $i_a i_B^{2/3} T_{eb}$.

This dependence leads to the following scaling law in grid structural failure given as

$$\frac{T_{sf}}{T_{sf0}} = \frac{i_{a0} i_{B0}^{2/3}}{i_a i_B^{2/3}} \tag{10}$$

where T_{sf} is a time for structural failure.

Summary

A scaling model for grid lifetime was presented for a 3-grid ion engine. The process for electron backstreaming was modeled with the space-charge-limited current density law and the extended effective acceleration length considering that the electron backstreaming determined the lifetime of the ion engine. All the parameters in the model can be obtained explicitly either by calculations or measurements. The characteristic of the model is that lifetime strongly depends on beam current and accel grid voltage. An evaluation was made to validate the model using a computer program and showed that the model agreed quite well with simulations and gave good scaling for grid lifetime.

References

[1] K. Komurasaki, Y. Arakawa and H. Takegahara, "An Overview of Electric and Advanced Propulsion Activities in Japan," 3rd International Conference on Spacecraft Propulsion (2000).

[2] J. M. Sankovic, and J. W. Dunning, "An Overview of Current NASA Activities in Electric Propulsion Technology," IEPC-99-003 (1999).

[3] G. Saccoccia, "European Activities Electric Propulsion," 3rd International Conference on Spacecraft Propulsion (2000).

[4] J. R. Brophy, J. E. Polk, and V. K. Rawlin, "Ion Engine Service Life Validation by Analysis and Testing," 32nd Joint Propulsion Conference and Exhibit, AIAA 96-2715, Lake Buena Vista, 1996.

[5] S. Shimada, K. Satoh, Y. Gotoh, E. Nishida, T. Noro, H. Takegahara, K. Nakamaru and H. Nagano, "Ion Thruster Endurance Test Using Development Model Thruster for ETS-VI," IEPC-93-169 (1993).

[6] R. A. Bond and P. M. Latham, "Ion Thruster Extraction Grid Design and Erosion Modeling using Computer Simulation," AIAA-95-2923 (1995).

[7] T. Shiraishi, H. Kuninaka, S. Satori, and K. Kuriki, "Numerical Simulation of Grid Erosion for Ion Thruster," Proceedings of the 24th International Electric Propulsion Conference, Vol.1, pp.586-594 (1995).

[8] M. Nakano and Y. Arakawa, "Ion Thruster Lifetime Estimation and Modeling Using Computer Simulation," IEPC-99-145 (1999).

[9] G. Aston, H. R. Kaufman, P. J. Wilbur, "Ion Beam Divergence Characteristics of Two-Grid Accelerator Systems," AIAA Journal, Vol.16, May 1978, No.5, pp.516-524.

[10] H. R. Kaufman, "Accelerator System Solutions for Broad-Beam Ion Sources," AIAA Journal, Vol.15, July 1977, pp.1025-34.

[11] Y. Yamamura, Y. Itikawa, N. Itoh, "Angular Dependence of Sputtering Yields of Monatomic Solids," IPPJ-AM-26, Institute of Plasma Physics, Nagoya University, (1983).

[12] I. Funaki, H. Kuninaka, Y. Shimizu, K. Toki, S. Satori and K. Nishiyama, "Verification Tests of 10-cm-diam. Carbon-Carbon Composite Grids for Microwave Discharge Ion Thruster," IEPC-99-164 (1999).